Journal of Medicinal Chemistry

Article

Novel Derivatives of Pyridylbenzo[*b*]thiophene-2-carboxamides and Benzo[*b*]thieno[2,3-*c*]naphthyridin-2-ones: Minor Structural Variations Provoke Major Differences of Antitumor Action Mechanisms

Katja Ester, Marijana Hranjec, Ivo Piantanida, Irena C#aleta, Ivana Jarak, Kres#imir Pavelic#, Marijeta Kralj, and Grace Karminski-Zamola

J. Med. Chem., **2009**, 52 (8), 2482-2492• DOI: 10.1021/jm801573v • Publication Date (Web): 30 March 2009

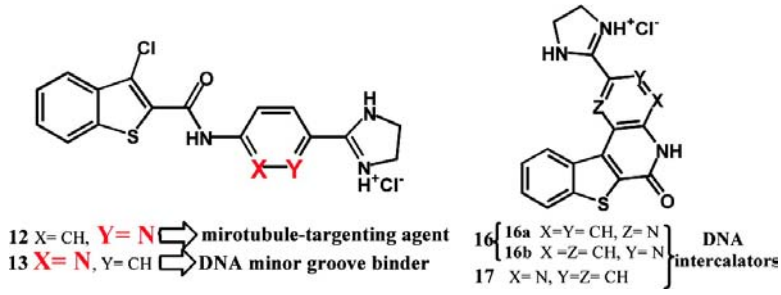

More About This Article

Additional resources and features associated with this article are available within the HTML version:

- Supporting Information
- Access to high resolution figures
- Links to articles and content related to this article
- Copyright permission to reproduce figures and/or text from this article

View the Full Text HTML

Journal of Medicinal Chemistry is published by the American Chemical Society.
1155 Sixteenth Street N.W., Washington, DC 20036

Novel Derivatives of Pyridylbenzo[*b*]thiophene-2-carboxamides and Benzo[*b*]thieno[2,3-*c*]naphthyridin-2-ones: Minor Structural Variations Provoke Major Differences of Antitumor Action Mechanisms

Katja Ester,[‡,†] Marijana Hranjec,[§,†] Ivo Piantanida,[||] Irena Ćaleta,[§] Ivana Jarak,[§] Krešimir Pavelić,[‡] Marijeta Kralj,*[,‡] and Grace Karminski-Zamola*[,§]

Division of Molecular Medicine, "Ruđer Bošković" Institute, Bijenička Cesta 54, P.O. Box 180, HR-10000 Zagreb, Croatia, Department of Organic Chemistry, Faculty of Chemical Engineering and Technology, University of Zagreb, Marulićev trg 20, P.O. Box 177, HR-10000 Zagreb, Croatia, and Division of Organic Chemistry and Biochemistry, "Ruđer Bošković" Institute, P.O. Box 180, HR-10002 Zagreb, Croatia

Received December 12, 2008

Novel cyano- and 2-imidazolinyl-substituted derivatives of pyridylbenzo[*b*]thiophene-2-carboxamides **4**, **5**, **10**−**13** and benzo[*b*]thieno[2,3-*c*]naphthyridin-2-ones **6**, **7**, **14**−**17** were prepared. All derivatives showed a prominent antiproliferative effect. Extensive DNA binding studies and additional biological evaluations point to various modes/targets of action. The results strongly support intercalation into DNA as a dominant binding mode of fused analogues, which was substantiated using topoisomerase I inhibition assay. Most intriguingly, only minor structural difference between "nonfused" compounds **12** and **13** has strong impact on the interactions with DNA; while **13** binds within the DNA minor groove in the form of dimer, **12** does not form significant interactions with DNA. The assumption that severe mitotic impairment (G2/M phase arrest) induced by **12** could point to tubulin, another important target, was confirmed by its obvious anti-tubulin activity observed in immunofluorescence assay, whereby treated cells showed disruption of microtubule formation comparable to the effect obtained by paclitaxel, a well-known tubulin antagonist chemotherapeutic.

Introduction

Classical chemotherapy using small molecules or bioactive natural products is still the mainstay of cancer treatment, whereby the major cellular targets are DNA and tubulin, along with various protein kinases.[1−3] Therefore, the everlasting search for novel small organic molecules with better activity and/or selectivity (primarily for the treatment of resistant tumor cells) is still of utmost importance for developing novel anticancer drugs. For example, quinolone is a common structure in alkaloids and its related compounds (e.g., substituted heterocyclic quinolones) exhibit several pharmacological activities and have therefore attracted considerable attention from medicinal and synthetic organic chemists.[3−7] Furthermore, naphthyridones, the isosteric counterparts of quinolones, and their derivatives have also been explored for their biological activity, such as antitumor activity[8,9] via inhibition of protein kinases[10,11] or topoisomerases[12−14] or tubulin inhibition[15] or antibacterial activity.[16−18]

As a part of our continuing search for potential anticancer agents related to heterocyclic quinolones (Figure 1), we have previously reported syntheses and strong inhibitory activities on several human cell lines of various cyano- or amidino-substituted benzo[*b*]thieno[2,3-*c*]quionolones and their "nonfused" analogues,[19−21] since it is well-known that amidines are structural parts of numerous compounds of biological interest as various medical and biochemical agents.[22−24] Amidino-substituted benzo[*b*]thieno[2,3-*c*]quinolones, strong ds-DNA/RNA intercalators, showed in general stronger and more selective antitumor activity than acyclic analogues, which did not intercalate at all. Because of the elucidating the impact of variation of thiophene vs benzene ring, we have also prepared amidino-substituted thieno[3′,2′:4.5]thieno[2,3-*c*]quinolones as well as their "nonfused" analogues, whereby both "fused" and "nonfused" analogues showed pronounced antitumor activity.[25]

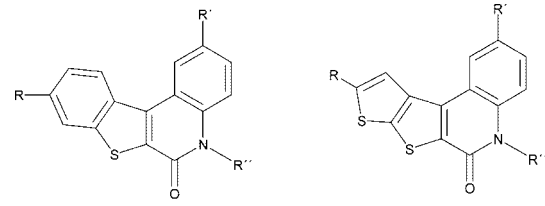

Figure 1. Structures of earlier prepared heterocyclic quinolones.[19−21,25]

Moreover, we recently reported the synthesis and antiproliferative action of amidino-substituted styryl-2-benzimidazoles and benzimidazo[1,2-*a*]quinolines, followed by amidino-substituted thienyl- and furylvinylbenzimidazoles and diazacyclopenta[*c*]fluorenes studies, which pointed toward imidazolinyl-substituted derivatives as the most active amidino-substituted analogues. The most promising compounds inhibited tumor growth, caused severe disturbance of the cell cycle and impairment in mitotic progression, and inhibited topoisomerases, which was related to their high DNA binding capacity.[26,27] All of the above-mentioned considerations prompted us to prepare novel 2-imidazolinyl-substituted derivatives of pyridylbenzo-[*b*]thiophene-2-carboxamides and benzo[*b*]thieno[2,3-*c*]naph-

* To whom correspondence should be addressed. For M.K.: phone, +385 1 4571 235; fax, +3851 4561 010; e-mail, marijeta.kralj@irb.hr. For G.K.-Z.: phone, ++38514597215; fax, ++38514597250; e-mail, gzamola@fkit.hr.

† These authors contributed equally to this work.

‡ Division of Molecular Medicine, "Ruđer Bošković" Institute.

§ University of Zagreb.

|| Division of Organic Chemistry and Biochemistry, "Ruđer Bošković" Institute.

10.1021/jm801573v CCC: $40.75
Published on Web 03/30/2009

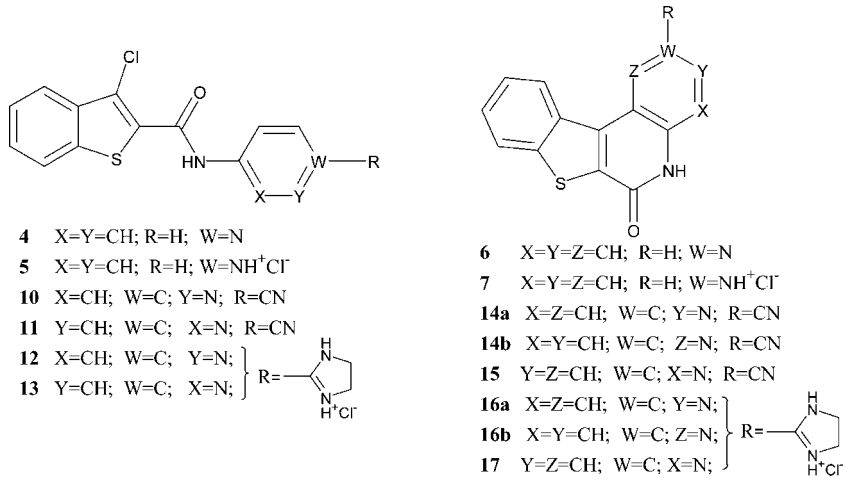

Figure 2. Unsubstituted (**4**−**7**), cyano- (**10**, **11**, **14**, **15**), and 2-imidazolinyl-substituted (**12**, **13**, **16**, **17**) derivatives of pyridylbenzo[*b*]thiophene-2-carboxamides and benzo[*b*]thieno[2,3-*c*]naphthyridin-2-ones.

Scheme 1. Synthesis of Pyridylbenzo[*b*]thiophene-2-carboxamides **4** and **5** and Benzo[*b*]thieno[2,3-*c*]naphthyridin-2-ones **6** and **7**

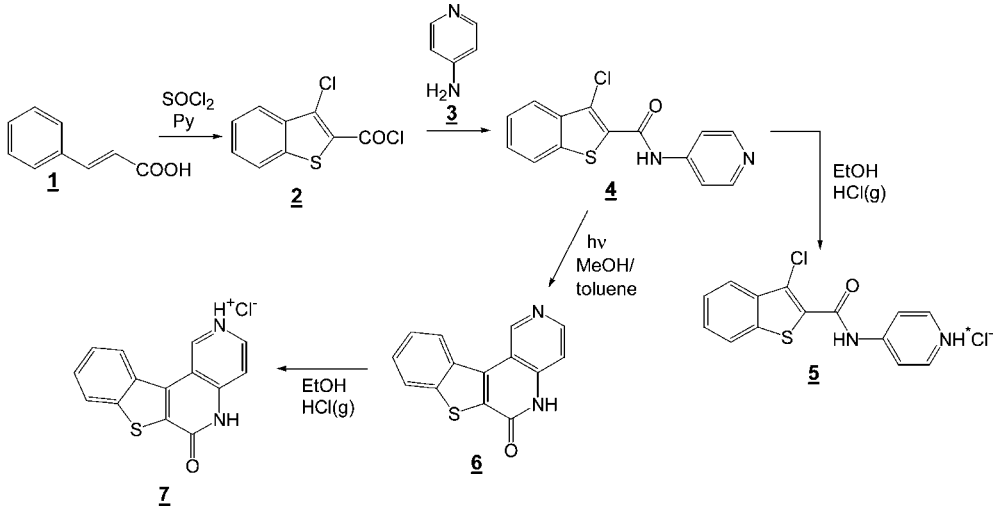

thyridin-2-ones and to explore their cellular targets that lead to their antiproliferative activity in more detail.

Chemistry

All compounds shown in Figure 2 were prepared according to Schemes 1 and 2. Starting from 3-chlorobenzo[*b*]thiophene-2-carbonyl chloride **2**, in the reaction with 4-aminopyridine **3**, 2-cyano-5-aminopyridine **8** and 2-amino-5-cyanopyridine **9**, the corresponding "nonfused" derivatives of pyridylbenzo[*b*]-thiophene-2-carboxamides **4**, **10**, and **11** were prepared. Cyano-substituted "nonfused" derivatives **10** and **11** gave in the Pinner reaction (conducted in either absolute ethanol or carbitol with ethylenediamine) 2-imidazolinyl-substituted pyridylbenzo[*b*]-thiophene-2-carboxamides **12** and **13** as hydrochloride salts. The hydrochloride salt **5** of compound **4** was prepared by protonation with the saturated ethanolic solution of gaseous HCl.

All fused derivatives of benzo[*b*]thieno[2,3-*c*]naphthyridin-2-ones **14**−**17** were prepared by photochemical dehydrohalogenation. The reaction was conducted in the mixture of methanol and toluene and followed by UV/vis spectroscopy. 2-Imidazolinyl-substituted "fused" derivatives **16** and **17** were prepared by two different methods: (a) from its cyano precursors **14** and **15** in the Pinner reaction; (b) by photochemical dehydrohalogenation reaction of "nonfused" 2-imidazolinyl-substituted derivatives of pyridylbenzo[*b*]thiophene-2-carboxamides **12** and **13**. There was no significant difference in the yields of above-mentioned preparation methods. "Nonfused" derivatives **10** and **12** gave, in the photochemical reaction, a mixture of two unseparable regioisomers **14a**,**b** and **16a**,**b**.

Spectroscopic Properties of Studied Compounds 12, 13, 16, and 17

Compounds studied in this paper could be divided into two groups with respect to flexibility and size of the condensed aromatic surface as follows: "nonfused" derivatives **4**, **5**, **10**−**13** and their "fused" derivatives **6**, **7**, **14**−**17**. Because of the structural similarity, we studied **12** and **13** as representatives of "nonfused" derivatives as well as **16** and **17** as representatives of "fused" derivatives. Aqueous solutions of **12**, **13**, **16**, and **17** were characterized by means of electronic absorption (UV/vis) and fluorescence emission spectroscopy (Supporting Information). Aqueous solutions of compounds **12**, **13**, **16**, and **17** were stable over 6 months. Because of the poor solubility of the studied compounds in water, stock solutions were prepared in DMSO (c(**12**) = 3.04 × 10^{-3} mol dm^{-3}; c(**13**) = 4.55 × 10^{-3} mol dm^{-3}; c(**16**) = 3.11 × 10^{-3} mol dm^{-3}; c(**17**) = 1.30 × 10^{-3} mol dm^{-3}), and in further experiments small aliquots of

Scheme 2. Synthesis of Cyano- (**10**, **11**, **14**, **15**) and 2-Imidazolinyl-substituted (**12**, **13**, **16**, **17**) Derivatives of Pyridylbenzo[*b*]thiophene-2-carboxamides and benzo[*b*]thieno[2,3-*c*]naphthyridin-2-ones

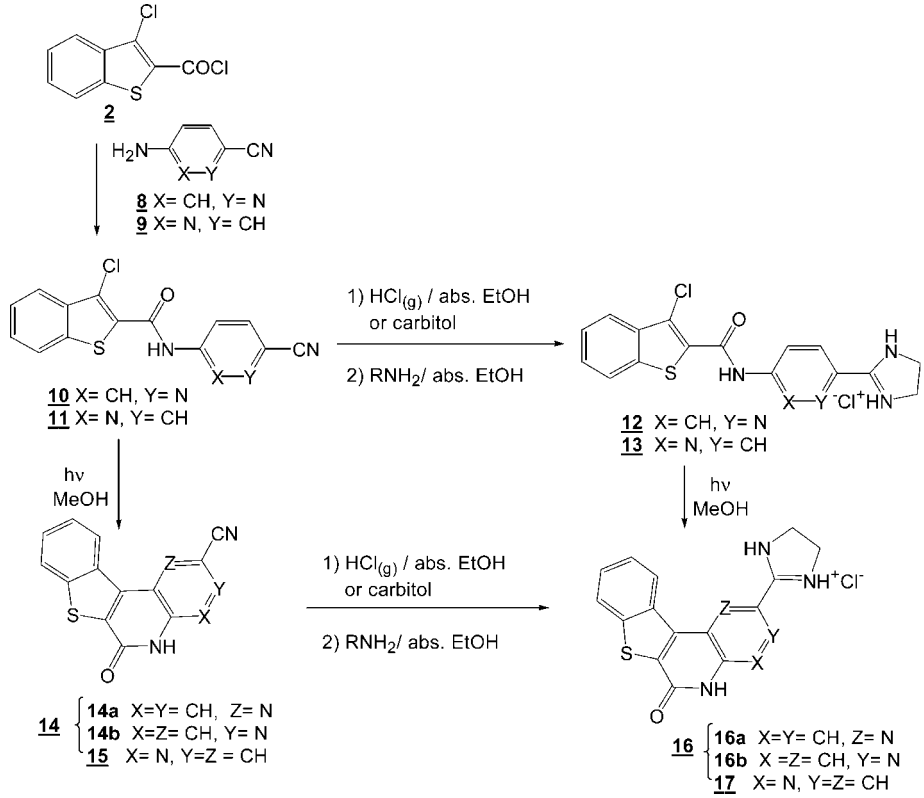

DMSO stock solutions were added into the aqueous medium, provided that the DMSO content in experiments was less than 1%.

Interaction of Compounds 12, 13, 16, and 17 with Calf Thymus (ct) DNA

UV/Visible and Fluorimetric Titrations. The UV/vis spectra of **13**, **16**, and **17** exhibited strong hypochromic changes (H(**13**) = 35%, H(**16**) = 24%, H(**17**) = 23%) as well as pronounced batochromic shifts ($\Delta\lambda$(**13**) = +9 nm, $\Delta\lambda$(**16**) = +9 nm, $\Delta\lambda$(**17**) = +12 nm) upon titration with ct-DNA (Figure 3 and Supporting Information), while for **12** only minor changes were observed. However, it was not possible to process UV/vis titration data of **16** and **17** by Scatchard equation,[28] since titrations were in better part done at excess of compound over DNA; at such conditions more different binding modes could be present, which was actually supported by opposite spectral changes dependent on the ratio $r_{[\text{compound}]/[\text{polynucleotide phosphate}]}$ as well as by deviation from isosbestic points. Only processing of UV/vis titration data obtained for **13** by Scatchard equation gave acceptable results (Table 1).

Strong fluorescence of **13**, **16**, **17** in aqueous medium allowed titrations to be done at an order of magnitude lower concentrations with respect to UV/vis experiments, thus enabling collection of many data points at high ct-DNA over compound excess. Addition of ct-DNA strongly quenched fluorescence of **13**, **16**, **17** (Figure 4), and processing of titration data by means of the Scatchard equation[28] for **16** and **17** resulted in excellent fitting of the experimental and calculated data for values of ratio $n_{[\text{bound compound}]/[\text{polynucleotide}]} = 0.2-0.3$, but for easier comparison log K_s values were recalculated for fixed $n = 0.2$ (Table 1).

Thermal Denaturation Experiments. In the thermal denaturation experiments addition of "nonfused" derivative **12** did not yield any measurable effect on the T_m value of ct-DNA, while its close analogue **13** yielded weak but measurable stabilization of the ct-DNA double helix (Table 2). The "fused"

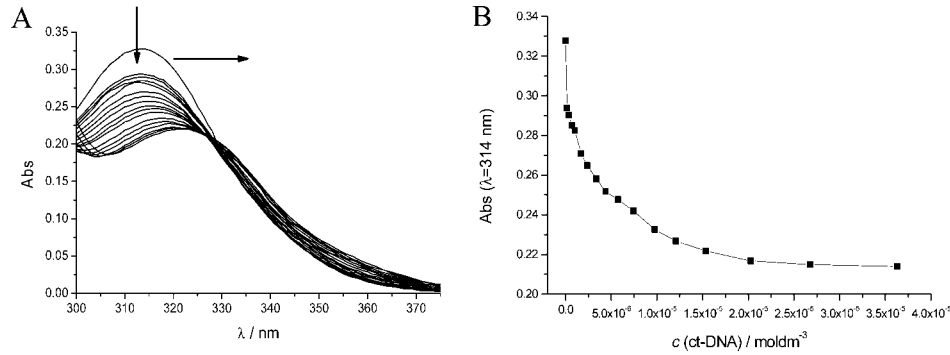

Figure 3. UV/vis titration of **13** ($c = 1.2 \times 10^{-5}$ mol dm^{-3}) with ct-DNA (A) and spectroscopic changes at $\lambda_{max} = 314$ nm as a function of ct-DNA concentration (B) at pH 7.0, buffer Na cacodylate, $I = 0.05$ mol dm^{-3}.

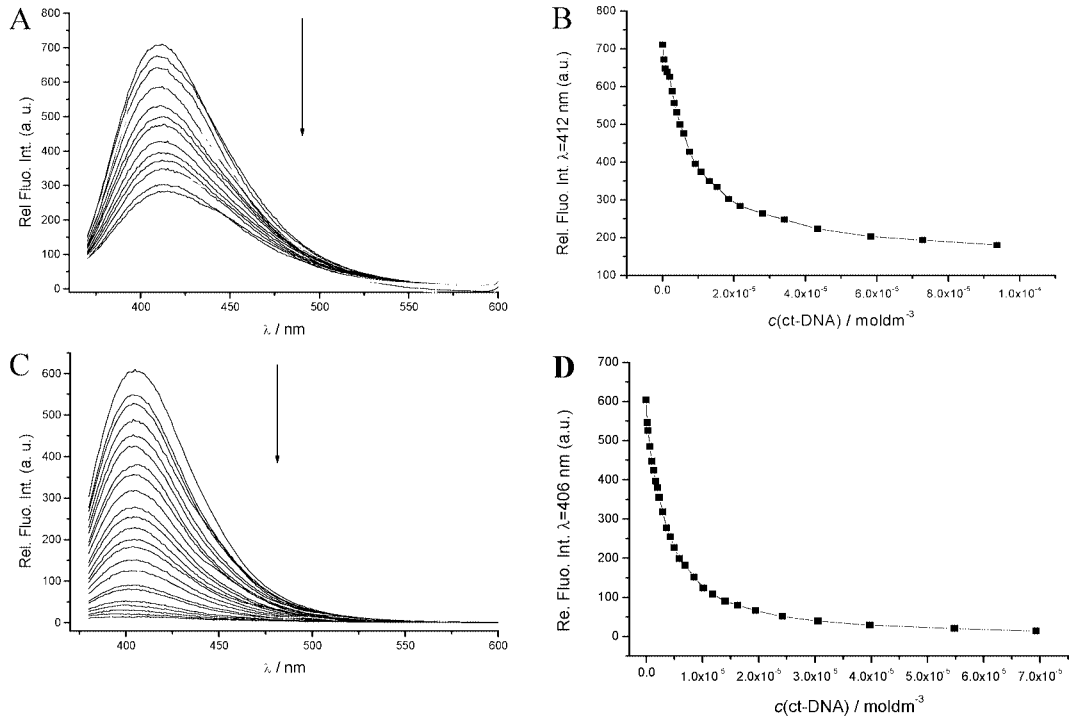

Figure 4. Fluorimetric titration with ct-DNA of nonfused compound **13**, $c = 1.9 \times 10^{-6}$ mol dm^{-3}, $t_{incub} = 3$ min (A); dependence of fluorescence intensity of **13** at $\lambda = 412$ nm on c(ct-DNA) (B); fused compound **17**, $c = 6.7 \times 10^{-7}$ mol dm^{-3}, $t_{incub} = 3$ min (C); dependence of fluorescence intensity of **17** at $\lambda = 406$ nm on c(ct-DNA) (D).

Table 1. Binding Constants (log K_s) and Ratios $n_{[\text{bound compound}]/[\text{polynucleotide phosphate}]}$[a] calculated from the UV/Visible[b] or Fluorimetric Titrations[c] with ct-DNA at pH 7.0 (Buffer Sodium Cacodylate, $I = 0.05$ mol dm^{-3})

	12	**13**	**16**	**17**
log K_s	*d*	5.6[c]/(5.7[b])	6.5[c]	6.44[c]
n	*d*	0.4[c]/(0.5[b])	0.2[c]	0.2[c]
Δ Int [e]	*d*	0.21	0.25[c]	0.001[c]

[a] Titration data were processed according to the Scatchard equation[28] for fixed ratio $n_{[\text{bound compound}]/[\text{polynucleotide}]} = 0.2$; Na cacodylate buffer, pH 7, $I = 0.05$ M. [b] UV/vis titration of **13** (Figure 3). [c] Fluorimetric titrations. [d] Not possible to calculate because of the weak fluorescence and negligible changes of UV/vis spectrum. [e] Change of fluorescence Δ Int = Int(complex)/Int(compound); values of Int(complex) were calculated by the Scatchard equation.

Table 2. ΔT_m Values of ct-DNA upon Addition of Different Ratios r [b] of **12**, **13**, **16**, **17** at pH 7.0 (Buffer Sodium Cacodylate, $I = 0.05$ mol dm^{-3})

	ΔT_m [a] (°C)			
r [b]	**12**	**13**	**16**	**17**
0.3	0	1.3	4.2	6.6
0.5	0.9	2.1	6.0	8.7

[a] Error in ΔT_m: ±0.5 °C. [b] r = [compound]/[polynucleotide].

derivatives **16** and **17** induced moderate stabilization effects accompanied by significant nonlinear dependence of ΔT_m values on the ratio r (Table 2).

CD Experiments. To get insight into the changes of polynucleotide properties induced by small molecule binding, we have chosen CD spectroscopy as a highly sensitive method toward conformational changes in the secondary structure of polynucleotides.[29] In addition, achiral small molecules like **12**, **13**, **16**, **17** can eventually acquire induced CD spectrum (ICD) upon binding to polynucleotides, from which mutual orientation of small molecule and polynucleotide chiral axis could be derived, consequently giving useful information about modes of interaction.[30]

The addition of studied compounds to the calf thymus DNA resulted in pronounced changes of the CD spectrum of ct-DNA (Figure 5). For compound **13** at conditions of higher ct-DNA excess over compound ($r_{[\mathbf{13}]/[\text{ct-DNA}]} = 0-0.2$), only minor changes in the CD spectrum with ct-DNA were observed. Most intriguingly, at $r = 0.3-1$ strong induced CD (ICD) bisignate exciton signal appeared at $\lambda > 280$ nm, characterized by a negative band at $\lambda = 295$ nm and a positive band at $\lambda = 316$ nm (Figure 5). The isoelliptic point at $\lambda = 305.6$ nm pointed toward the presence of only two spectroscopicaly active species. Since compound **13** does not have any intrinsic CD spectrum, such a strong bisignate exciton ICD signal most likely resulted from two molecules of **13** forming a dimer within the minor groove of ct-DNA.[29,31] Unlike **13**, compound **12** induced uniform changes within the complete range of $r = 0-1$, namely, weak decrease of the DNA band at $\lambda = 280$ nm as well as an increase of positive ICD band at $\lambda = 320$ nm. Such an ICD band is typical for binding of single molecules within the DNA minor groove.[31] Furthermore, changes of the CD spectrum of ct-DNA induced by fused analogues **16** and **17** were substantially different. Compound **17** yielded only a decrease of DNA bands at $\lambda = 245$ and 280 nm, pointing toward disruption of DNA double helix chirality. Its close analogue **16** also yielded a decrease of the DNA band at $\lambda = 245$ nm characteristic of elongation of phosphate backbone. At variance to **17**, compound **16** yielded an increase of the band at $\lambda = 280$ nm and appearance of a new, weak, negative band at about $\lambda = 303$ nm. Since **16** does not have any intrinsic CD spectrum, observed changes could be attributed to the ICD spectrum of intercalated molecule of **16**, its longer axis being coplanar with longer axes of DNA base pairs.[31] Absence of any measurable ICD band in the case of the **17**/DNA complex does not exclude the intercalative binding mode, since it could be the consequence of more different orientations of intercalated molecule with respect to the longer axes of DNA base pairs.[29−31]

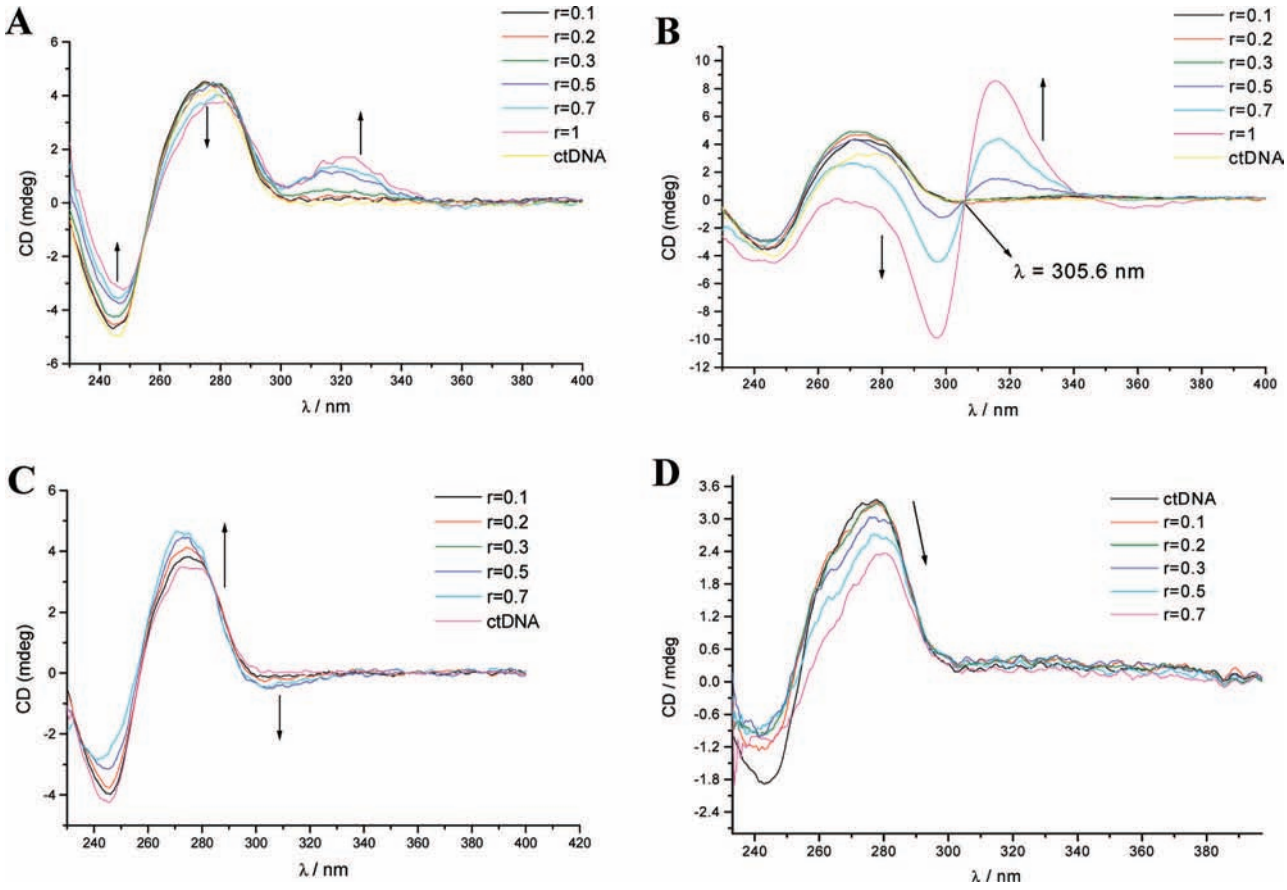

Figure 5. CD titrations of ct-DNA ($c = 4.0 \times 10^{-5}$ mol dm^{-3}) with **12** (A), **13** (B), **16** (C), and **17** (D), ratios $r_{[12,13]/[\text{ct-DNA}]} = 0-1$ and $r_{[16,17]/[\text{ct-DNA}]} = 0-0.7$, at pH 7 (Na cacodylate buffer, $I = 0.05$ mol dm^{-3}).

Viscometry. Viscometry experiments (Supporting Information) yielded values of α(**16**) = 0.74 and α(**17**) = 0.76, which differ from the value obtained for ethidium bromide (α(EB) = 0.84) by the error of the method ($\alpha \pm 0.1$). Obtained values strongly support intercalation of **16** and **17** into ds-DNA as the dominant binding mode. On the other hand, addition of "nonfused" analogues (**12**, **13**) resulted in significantly smaller viscosity changes and even reduced DNA solution viscosity (Supporting Information), which does not support the intercalative binding mode.

Discussion of Interactions with ct-DNA

According to the spectrophotometric titrations and especially thermal denaturation experiments, interactions of "nonfused" derivative **12** within the ct-DNA minor groove under biologically relevant conditions are negligible. On the other hand, all applied methods revealed significantly different behavior of nonfused analogue **13**, pointing toward its considerable affinity toward ct-DNA as well as measurable thermal stabilization of DNA double helix. In addition, CD experiments revealed that at high ratio *r*, **13** binds to ct-DNA minor groove as dimer, which is not the case for **12**. Most intriguingly, only a minor structural difference between compounds **12** and **13** (position of heterocyclic nitrogen with respect to the amidine substituent; for **12** it is in the ortho position, and for **13** it is in the meta position) seems to have exceptionally strong impact on the interactions with DNA.

The values of the binding constants (log K_s) as well as effects in the UV/vis spectra obtained for "fused" analogues (**16** and **17**) are quite similar to those of "nonfused" analogue **13**. However, ΔT_m values induced by **16** and **17** are significantly higher than those found for **13**. Furthermore, CD and viscometry experiments revealed different binding sites for **13** (DNA minor groove), **16**, and **17** (intercalation). Such difference in binding mode can be attributed to the significantly smaller aromatic surface of the "nonfused" analogue (**13**) if compared to the fused **16** and **17**, whose large, planar aromatic surface strongly preferred intercalation into DNA as a dominant binding mode.

Table 3. In Vitro Inhibition of Compounds **5**−**17** on the Growth of Tumor Cells

	IC$_{50}$ (μM)[a]				
compd	H460	HeLa	MiaPaCa-2	SW620	MCF-7
5	68 ± 10	2 ± 0.5	38 ± 4	38 ± 4	51 ± 49
7	>100	14 ± 8	7 ± 7	6 ± 4	>100
11	59 ± 40	2 ± 0.4	8 ± 2	20 ± 11	20 ± 4
12	1.3 ± 0.1	1 ± 0.3	1.6 ± 0.1	1.3 ± 0.2	4 ± 1
13	1 ± 0.6	1.5 ± 0.1	1 ± 0.3	1 ± 0.3	1.8 ± 0.2
15	>100	7 ± 5	12 ± 2	22 ± 20	45 ± 17
16	1.3 ± 0.0	0.6 ± 0.5	0.3 ± 0.1	0.2 ± 0.2	2 ± 0.6
17	1 ± 0.1	1.7 ± 0.1	1 ± 0.2	0.6 ± 0.4	1.6 ± 0.2

[a] IC$_{50}$: the concentration that causes a 50% reduction of the cell growth.

Biological Results and Discussion

Compounds **5**, **7**, **11**−**13**, **15**−**17** were screened for their potential antiproliferative effects on a panel of five human cell lines, which were derived from different cancer types including HeLa (cervical carcinoma), MCF-7 (breast carcinoma), SW620 (colon carcinoma), MiaPaCa-2 (pancreatic carcinoma), and H460 (lung carcinoma) (Table 3 and Figure 6).

All of the compounds showed a strong growth inhibitory effect. Compounds **5**, **7**, **11**, and **15** were active in the micromolar range, with higher specificity toward HeLa cells.

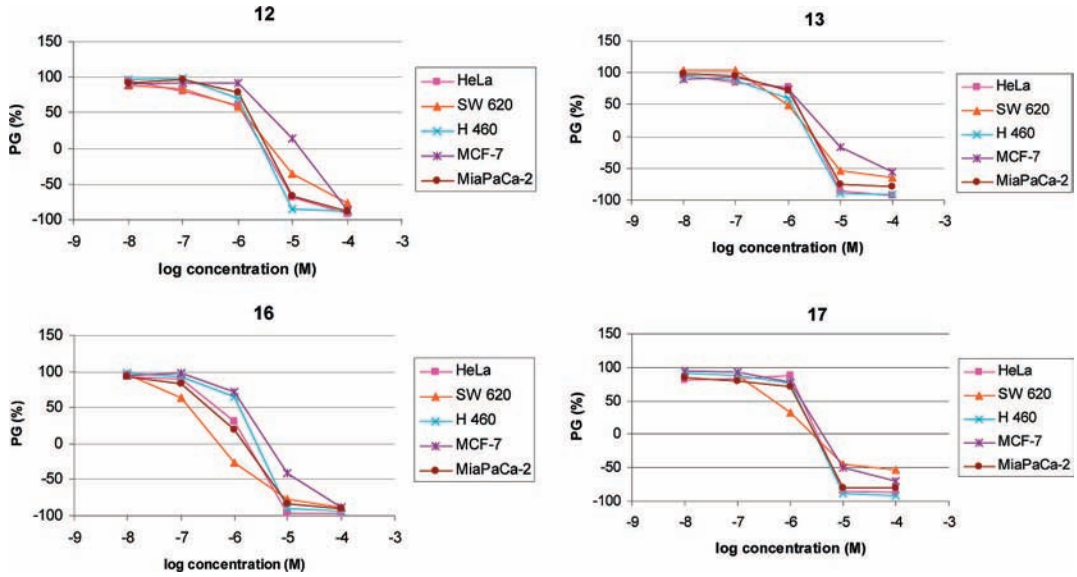

Figure 6. Concentration−response profiles for the representative nonfused (**12** and **13**) and fused (**16** and **17**) analogues tested on various human cell lines in vitro. The cells were treated with the compounds at different concentrations, and percentage of growth (PG) was calculated. Each point represents a mean value of four replicates in three individual experiments.

An even more prominent effect was displayed by compounds **12**, **13**, **16**, and **17**. The most active compound **16** was active in the submicromolar range, with special selectivity to MiaPaCa-2, HeLa, and SW 620 cells. The high activity of tested compounds was in agreement with our previous results,[26,27] which implied that imidazolinyl-substituted derivatives were highly active. Nevertheless, our previous results indicated that "fused" derivatives were more effective than their "nonfused" analogues, while in the present study both "nonfused" and "fused" compounds had similar, major antiproliferative effect.

Interestingly, the above-mentioned DNA binding data suggest that a strong growth inhibitory effect, represented by both "fused" and "nonfused" derivatives, may involve different molecular mechanisms. For instance, since fused derivatives were shown to be DNA intercalators, their high activity was expected. Similarly, nonfused compound **13** binds as a dimer to DNA minor groove, pointing also to DNA as the dominant target for its antiproliferative action. However, quite unexpectedly, its close analogue **12**, which does not interact with DNA under biologically relevant conditions, reveals that besides noncovalent interactions with DNA, another, different mechanism/target should be responsible for its prominent activity. Therefore, we performed additional experiments to give an insight to more detailed antiproliferative mechanisms or targets.

Cell Cycle Perturbations. Consistent with our previously published results,[26,27] we also expected significant disturbance in the cell cycle induced by the here-presented compounds. We selected compounds **12**, **13**, **16**, and **17** as the most active representatives of "nonfused" and "fused" analogues that, as discussed earlier, showed interesting and different DNA binding features. All compounds were tested for cell cycle perturbation on MiaPaCa-2 cell line for 24 and 48 h using flow cytometry. Concentration that was used (5 μM) was slightly higher than IC_{50} of all compounds (Figure 7). All of the compounds induced statistically significant accumulation of cells in the G2/M phase of the cell cycle. Compound **16**, the fused analogue, induced strong G2/M arrest, as expected by its high antiproliferative activity and strong intercalation into double stranded DNA. On the other hand, compounds **13** and **17** displayed rather moderate effect on the cell cycle perturbations, with an increase in the G2/M and a decrease in G0/G1 population at 24 h, while this

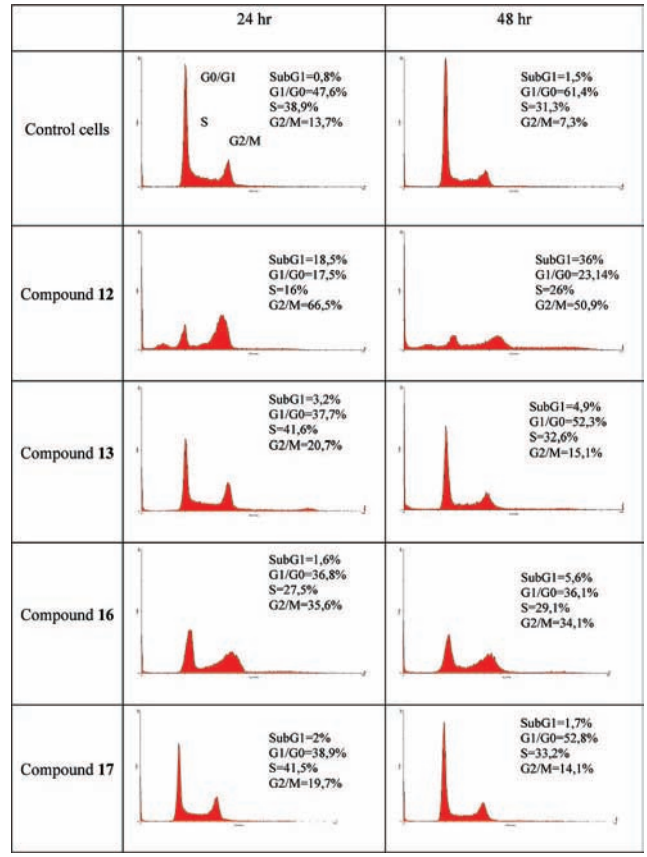

Figure 7. DNA histograms obtained by flow cytometry (see Experimental Section) and the percentages of cells in sub G1 (apoptotic cells), G0/G1, S, and G2/M cell cycle phases, after the treatment of MiaPaCa-2 cells with **12**, **13**, **16**, and **17** (all at 5 μM) for 24 and 48 h. The *x* axis represents the DNA content, while the *y* axis represents the number of events (cells).

effect afterward diminished. The G2/M delay induced by these compounds was surely the consequence of interactions with DNA that indirectly led to the DNA damage. To confirm the influence of such interactions on cellular functions related to DNA, especially in light of our previous results,[26,27] we

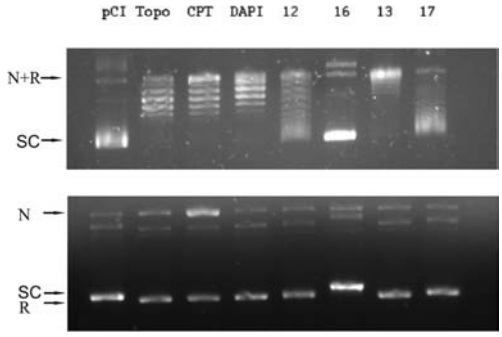

Figure 8. Influence of selected test compounds on relaxation of plasmid DNA by topoisomerase I. DNA samples were separated by electrophoresis on an agarose gel without (upper gel) or containing (lower gel) ethidium bromide, respectively: native supercoiled pCI DNA (0.4 μg) substrate in the assay buffer alone (lane pCI), incubated with topoisomerase I (3 U) (lane Topo) or in combination with control drug−camptothecin (100 μM) (lane CPT), DAPI (100 μM) (lane DAPI), and selected test compounds **12**, **13**, **16**, and **17** (200 μM each).

additionally investigated whether intercalation or minor groove binding would interfere with topoisomerase I activity. Despite the high DNA binding potential, none of the three compounds that intercalate (**16** and **17**) or bind to the minor groove (**13**) caused a measurable amount of subG0/G1 population representing apoptotic cells.

Interestingly, compound **12**, which binds weakly to DNA, induced the most severe G2/M arrest together with the reduction of cell number in the G0/G1 and S phases at both time points. Also, an increase in the percentage of apoptotic cells was observed. Strong antiproliferative effect, followed by severe G2 or mitotic arrest and apoptosis displayed by **12**, which does not bind to DNA under biologically relevant conditions, directed us toward the possibility that this analogue may interfere with the cellular tubulin level, since similar observations were also reported by other groups[1,3,32,33] showing that microtubule-targeted tubulin-polymerizing agents induce cell cycle G2/M phase delay and mitotic arrest of cancer cells. In other words, G2/M arrest of the cell cycle may be the result of several stresses, such as tubulin-binding agents and DNA damage stress. Therefore, we also performed cellular tubulin staining using immunoflourescence.

Topoisomerase I DNA Unwinding/Cleavage Assay. To elucidate whether tested compounds act as topoisomerase inhibitors, we employed in vitro assay using purified topoisomerase I from calf thymus. As described in the Experimental Section, this assay allows discriminating between nonspecific (due to intercalation) and specific (poisoning) effect on topoisomerase I by separation of various forms of plasmid DNA in agarose gels either without or containing ethidium bromide (Figure 8). Namely, by comparing both gels, we were able to clearly distinguish among nicked (open circular), supercoiled, and relaxed forms of plasmid DNA.[27,34,35] Figure 8 clearly shows that camptothecin (CPT) as a potent poison of topoisomerase I strongly induced nicking of plasmid DNA, which can be seen as an increased intensity of the nicked open circular DNA band (cleavage product). As the minor groove binder representative, we selected DAPI (4′,6-diamidino-2-phenylindole), which was shown to be inactive in our assay where only the relaxed form of the plasmid is present. Although some of the known groove binders act as topoisomerase I poisons,[36,37] many of them do not interfere with enzyme functions, and our analogue (**13**) also did not have any effect similar to DAPI. As expected, compound **12** confirmed its weak affinity toward DNA in our assay, where no major interference with enzyme was present. Compounds **16** and **17** inhibited the relaxation of supercoiled DNA but did not induce nicking of DNA, representing a pattern typical for intercalators as ethidium bromide (EtBr).[27] The compound **16** induced a bit stronger shift in the mobility of supercoiled plasmid than **17**, resulting probably from a somewhat better solubility of **16** compared to **17** at 200 μM. Namely, intercalators locally unwind DNA, thus inducing resupercoiling of the plasmid DNA as a consequence of a decrease in DNA linking number that accompanies relaxation by the enzyme. Moreover, the resupercoiling is often followed by a strong shift in the mobility of supercoiled plasmid. The observed phenomenon occurs in a dose-dependent manner and depends on the extent to which the intercalator molecule was bound.[34,35,37]

Inhibition of DNA relaxation by the enzyme seems to be a coincidence of intercalation into DNA; thus, **16** and **17** act as nonspecific topoisomerase I catalytic inhibitors. In general, topoisomerase I assay data confirmed the nature of DNA binding by all compounds.

Cellular Tubulin Staining. The potency of the compound **12** to disrupt microtubule formation was determined by immunofluorescence microscopic examination, as described in the Experimental Section. MiaPaCa-2 cells treated with **12** showed severely disrupted cell shape and tubulin network (Figure 9). Furthermore, multinucleation and subsequent fragmentation of cell nucleus were present, as shown by DAPI staining. When our compound was compared to the well characterized anti-tubulin drug paclitaxel,[2,38] the effect was strikingly similar. Other compounds did not alter cellular or nuclear shape in such a manner, although more severe morphological changes, along with nuclear fragmentation, were observed by other compounds, especially **16** (Supporting Information). This was the expected consequence of severe DNA damage that resulted in mitotic delay leading probably toward mitotic catastrophe, one of the common death responses to DNA damaging agents of tumor cells with p53 mutated gene, such as MiaPaCa-2 cell line.[39] Interestingly, only compound **12** induced apoptosis, as obtained by flow cytometry. This is in perfect accordance with the literature data, which reveal that the p53 gene status is one of the main determinants of tumor cells' response to various chamotheraputics, whereby mutational loss of function of the p53 tumor suppressor mostly confers resistance toward DNA-damaging anticancer agents because of their inability to activate apoptosis (as discussed above). On the other hand, as reviewed by Bhalla,[33] the status of the p53 gene is dispensable for the sensitivity to microtubule-targeting agents, which can readily activate apoptosis in a p53-independent manner, which may explain the observed result. Although we were not able to determine the precise mechanism of tubulin disruption that was obtained by **12**, significant alteration of microtubule formation is clearly confirmed.

Conclusions

This study represents the synthesis of novel 2-imidazolinyl-substituted derivatives of pyridylbenzo[*b*]thiophene-2-carboxamides and benzo[*b*]thieno[2,3-*c*]naphthyridin-2-ones as hydrochloride salts. All studied compounds exhibited a strong growth inhibitory effect, especially compounds **12**, **13**, **16**, and **17**, which were active in the low micromolar range, and therefore, they were submitted to further evaluations. Spectroscopic analysis of compounds/DNA interactions showed that only a minor structural difference between compounds **12** and **13** (position of heterocyclic nitrogen with respect to the amidine substituent) seems to have exceptionally strong impact on the interactions with DNA, revealing that compound **13**, in the form of dimer, binds to DNA minor groove while compound **12** does not interact with DNA under biologically relevant conditions. Both "fused" derivatives (**16** and **17**) bind to DNA as interca-

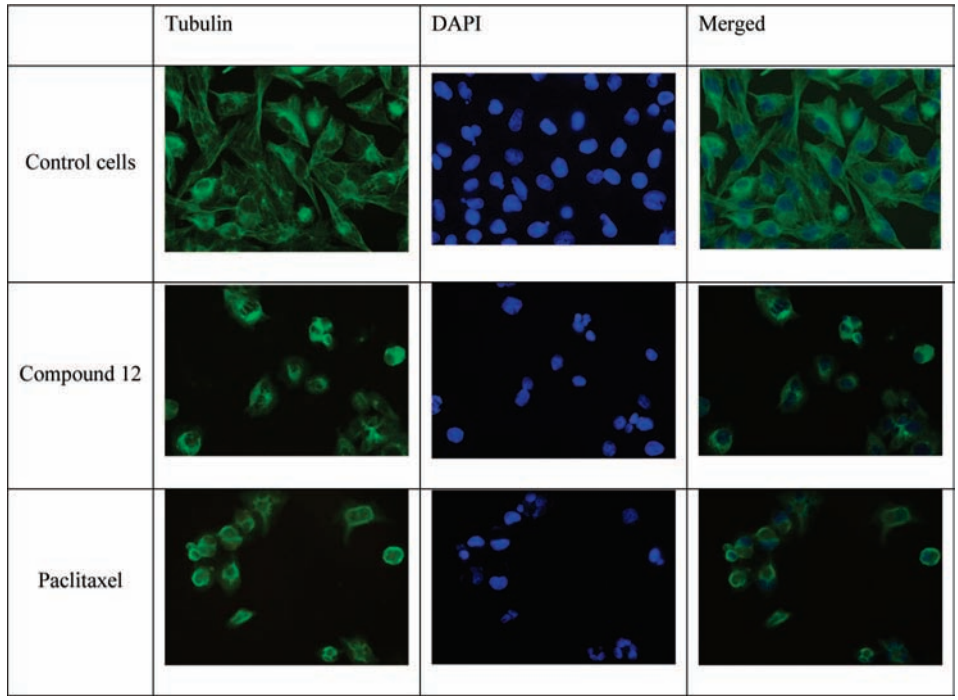

Figure 9. Tubulin immunofluorescence staining of MiaPaCa-2 cells. Coverslips containing MiaPaCa-2 cells were incubated with compound **12** (5 μM) and paclitaxel (1nM) for 24 h and then stained with anti-α-tubulin antibody, FITC-conjugated secondary antibody, and DAPI. Magnification is 400×.

lators, which was also substantiated by topoisomerase I inhibition assay, confirming that they act as topoisomerase I catalytic inhibitors. Cell cycle study showed G2/M delay by all compounds, which could be a consequence of several stresses, such as tubulin-binding agents and DNA damage stress. Interestingly, compound **12** had the most potent effect on the cell cycle, pointing toward tubulin as another cellular target besides DNA. Indeed, following immunofluorescence staining, we confirmed significant alteration of microtubule formation by compound **12**. In conclusion, the here-presented novel compounds possess high potential as novel leads with anticancer potentials; however, the most intriguing result is the observation that only a minor structural difference between derivatives **12** and **13** results in the major difference in their targets/mechanisms of action.

Experimental Section

Chemistry. Melting points were determined on a Koffler hot stage microscope and are uncorrected. IR spectra were recorded on Nicolet magna 760, Perkin-Elmer 297, and Perkin-Elmer Spectrum 1 spectrophotometers, with KBr disks. ^{1}H and ^{13}C NMR spectra were recorded on Varian Gemini 300, Bruker Avance DPX 300, and Bruker Avance DRX 500 spectrometers using TMS as an internal standard in DMSO-d_6. Elemental analyses for carbon, hydrogen, and nitrogen were performed on a Perkin-Elmer 2400 elemental analyzer and a Perkin-Elmer series II CHNS analyzer 2400. Where analyses are indicated only as symbols of elements, analytical results obtained are within 0.4% of the theoretical value. In preparative photochemical experiments the irradiation was performed at room temperature with a water-cooled immersion well with an "Origin Hanau" 400 W high pressure mercury arc lamp using Pyrex glass as a cutoff filter of wavelengths below 280 nm. All compounds were routinely checked by TLC with Merck silica gel 60F-254 glass plates.

Compounds 4−7, 10, 11. The synthesis procedures for compounds **4**−**7**, **10**, **11** are given in Supporting Information.

Synthesis of 3-Chlorobenzo[*b*]thiophene-*N*-[6-(2-imidazolinyl)pyridin-3-yl]-2-carboxamide Hydrochloride (12) and 3-Chlorobenzo[*b*]thiophene-*N*-[5-(2-imidazolinyl)pyridin-2-yl)-2-carboxamide Hydrochloride (13). A stirred suspension of the corresponding nitrile (**10**, **11**) in absolute ethanol or carbitol was cooled in an ice−salt bath and was saturated with HCl gas. The flask was then tightly stoppered, and the mixture was maintained at room temperature until the nitrile band disappeared (monitored by IR analysis at 2200 cm^{-1}). The reaction mixture was purged with N_2 gas and diluted with diethyl ether. The crude imidate was filtered off and was immediately suspended in absolute ethanol. Ethylenediamine was added and the mixture was stirred at reflux for 24 h. The crude product was then filtered off, washed with diethyl ether to give a white powder which was suspended in absolute ethanol and saturated with HCl (g). Reaction mixture was stirred at room temperature for 24 h. The products were filtered off and recrystallized from ethanol.

The yield on compound **12** (white powder, mp 215−219 °C) was 25.6%. ^{1}H NMR (DMSO-d_6) (δ ppm): 11.30 (s, 1H, NH_{amide}), 10.74 (bs, 2H, $NH_{amidine}$), 9.15 (s, 1H, H_{Py}), 8.49 (d, 1H, J = 6.9 Hz, H_{Py}), 8.31 (d, 1H, J = 8.6 Hz, H_{arom}), 8.24−8.15 (m, 2H, H_{arom}, H_{Py}), 8.02−7.93 (m, 2H, H_{arom}), 4.03 (s, 4H, $CH_{2imidazolyl}$). ^{13}C NMR (DMSO-d_6) (δ ppm): 163.5 (s), 144.5 (d), 139.7 (s), 139.0 (s), 137.2 (s), 133.8 (s), 132.3 (d), 129.6 (d), 129.0 (d), 128.9 (s), 127.9 (d), 125.1 (d), 124.9 (d), 122.7 (s), 119.2 (s), 45.9 (t, 2C).

The yield on compound **13** (white powder, mp >300 °C) was 30%. ^{1}H NMR (DMSO-d_6) (δ ppm): 11.34 (s, 1H, NH_{amide}), 11.02 (s, 2H, $H_{amidine}$), 9.13 (s, 1H, H_{Py}), 8.56 (d, 1H, J = 6.9 Hz, H_{Py}), 8.33 (d, 1H, J = 8.8 Hz, H_{arom}), 8.20−8.17 (m, 1H, H_{arom}), 7.97 (d, 1H, J = 7.0 Hz, H_{Py}), 7.66−7.63 (m, 2H, H_{arom}), 4.02 (s, 4H, $CH_{2imidazolyl}$). ^{13}C NMR (DMSO-d_6) (δ ppm): 165.0 (s), 157.6 (s), 154.6 (d), 144.8 (d), 138.7 (s), 137.2 (s), 136.8 (s), 131.1 (s), 129.9 (d), 128.6 (d), 124.2 (d), 123.9 (d), 120.0 (s), 116.6 (d), 109.0 (s), 46.0 (t, 2C).

Synthesis of Benzo[*b*]thieno-1*H*-[1,5]naphthyridin-2-one-6-(4,5-dihydro-1*H*-imidazol-2-yl) Hydrochloride (16a), Benzo[*b*]-thieno-1*H*-[1,7]naphthyridin-2-one-6-(4,5-dihydro-1*H*-imidazol-2-yl) Hydrochloride (16b), and Benzo[*b*]thieno-1*H*-[1,8]naphthyridin-2-one-6-(4,5-dihydro-1*H*-imidazol-2-yl) Hydrochloride (17). Method A. A stirred suspension of corresponding cyano substituted derivatives **14**, **15** in absolute ethanol was cooled in an ice−salt bath and was saturated with HCl gas. The flask was then tightly stoppered, and the mixture was maintained at room temperature until the nitrile band disappeared (monitored by IR analysis at 2200 cm^{-1}). The reaction mixture was purged with N_2

gas and diluted with diethyl ether. The crude imidate was filtered off and was immediately suspended in absolute ethanol. Ethylenediamine was added, and the mixture was stirred at reflux for 24 h. The crude product was then filtered off, washed with diethyl ether to give a white powder which was suspended in absolute ethanol and saturated with HCl(g). The reaction mixture was stirred at room temperature for 24 h. The crude product was filtered off and washed with a small amount of diethyl ether to give the corresponding products.

Method B. A solution of acyclic imidazolinyl-substituted pyridyl-3-chlorobenzo[*b*]thiophene-2-carboxamides **12**, **13** in ethanol/methanol was irradiated at room temperature. The reaction mixture was concentrated under the reduced pressure and the obtained solid was filtered off and recrystallized from methanol to give products.

16a and 16b. The yield of unseparable regioisomers **16a** and **16b** (yellow powder, mp >300 °C) was 64.5% (method A) and 89.3% (method B).

16a. ^{1}H NMR (DMSO-d_6) (δ ppm): 13.35 (s, 1H, NH_{amide}), 11.26 (bs, 2H, $NH_{amidine}$), 9.69 (d, 1H, $J = 7.8$ Hz, H_{arom}), 9.20 (s, 1H, $H_{naphthyr}$), 8.98 (s, 1H, $H_{naphthyr}$), 8.55 (d, 1H, $J = 7.8$ Hz, H_{arom}), 8.28 (d, 1H, $J = 7.7$ Hz, H_{arom}), 7.98 (d, 1H, $J = 7.7$ Hz, H_{arom}), 4.10 (bs, 4H, $H_{imidazolyl}$). ^{13}C NMR (DMSO-d_6) (δ ppm): 166.8 (s), 165.2 (s), 157.1 (s), 152.7 (s), 152.0 (s), 149.5 (s), 145.0 (s), 144.1 (d), 143.9 (d), 141.6 (s), 133.9 (s), 131.6 (d), 130.0 (d), 129.7 (d), 128.1(d), 46.3 (t, 2C).

16b. ^{1}H NMR (DMSO-d_6) (δ ppm): 13.10 (s, 1H, NH_{amide}), 11.08 (bs, 2H, $NH_{amidine}$), 9.36 (d, 1H, $J = 7.2$ Hz, $H_{naphthyr}$), 9.32 (d, 1H, $J = 7.3$ Hz,, $H_{naphthyr}$), 9.20 (d, 1H, $J = 7.7$ Hz, H_{arom}), 8.46 (d, 1H, $J = 7.8$ Hz, H_{arom}), 7.79−74.81 (m, 2H, H_{arom}), 4.10 (bs, 4H, $H_{imidazolyl}$). ^{13}C NMR (DMSO-d_6) (δ ppm): 167.0 (s), 165.9 (s), 156.0 (s), 152.1 (s), 151.3 (s), 149.6 (s), 144.9 (s), 144.1 (d), 144.0 (d), 141.1 (s), 132.4 (s), 130.7 (d), 130.1 (d), 129.3 (d), 128.6 (d), 46.1 (t, 2C).

17. The yield on **17** (white powder; mp >300 °C) was 43% (method A) and 56% (method B). ^{1}H NMR (DMSO-d_6) (δ ppm): 13.11 (s, 1H, NH_{amide}), 11.20 (bs 2H, $H_{amidine}$), 9.32 (s, 1H, $H_{naphthyr}$), 9.17 (s, 1H, $H_{naphthyr}$), 9.12 (dd, 1H, $J = 7.1$ Hz, $J = 6.7$ Hz, H_{arom}), 8.26 (dd, 1H, $J = 7.1$ Hz, $J = 6.7$ Hz, H_{arom}), 8.10−7.98 (m, 2H, H_{arom}), 4.10 (bs, 4H, $CH_{2imidazolyl}$). ^{13}C NMR (DMSO-d_6) (δ ppm): 166.1 (s), 165.8 (s), 155.0 (s), 152.6 (s), 150.9 (s), 148.4 (s), 146.0 (s), 144.2 (d), 143.9 (d), 140.1 (s), 132.6 (s), 130.2 (d), 130.0 (d), 129.2 (d), 128.8 (d), 46.8 (t, 2C).

Spectroscopy. The electronic absorption spectra were recorded on Varian Cary 50 and Varian Cary 100 Bio spectrometers and CD spectra on Jasco J815, in all cases using quartz cuvettes (1 cm). Fluorescence emission spectra were recorded on Varian Eclipse fluorimeter (quartz cuvettes, 1 cm), from 350 to 550 nm. The sample concentration in fluorescence measurements had an optical absorbance below 0.05 at the excitation wavelength. Under the experimental conditions used the absorbance and fluorescence intensities of studied compounds were proportional to their concentrations, while none of studied compounds showed a CD spectrum. The measurements were performed in the aqueous buffer solution (pH 7.0, sodium cacodylate buffer, $I = 0.05$ mol dm^{-3}).

Interactions with DNA. The calf thymus DNA (ct-DNA) was purchased from Aldrich, dissolved in the sodium cacodylate buffer, $I = 0.05$ mol dm^{-3}, pH 7.0, additionally sonicated, and filtered through a 0.45 μm filter, and the concentration of the corresponding solution was determined spectroscopically as the concentration of phosphates.[40] The measurements were performed in aqueous buffer solution (pH 7.0, sodium cacodylate buffer, $I = 0.05$ mol dm^{-3}).

Spectroscopic titrations were performed by adding portions of polynucleotide solution into the solution of the studied compound. The stability constant (K_s) and [bound compound]/[polynucleotide phosphate] ratio (n) were calculated according to the Scatchard equation[28] by nonlinear least-squares fitting, giving excellent correlation coefficients (>0.999) for K_s and n.

Thermal denaturation curves for ct-DNA and its complexes with studied compounds were determined as previously described by following the absorption change at 260 nm as a function of temperature. The absorbance of the ligand was subtracted from every curve, and the absorbance scale was normalized. The obtained T_m values are the midpoints of the transition curves, determined from the maximum of the first derivative or graphically by a tangent method. Given ΔT_m values were calculated by subtracting T_m of the free nucleic acid from T_m of complex. Every ΔT_m value here reported was the average of at least two measurements, and the error in ΔT_m is ±0.5 °C.

Viscometry experiments were conducted with an Ubbelohde microviscometer system. The temperature was maintained at 25 ± 0.1 °C. Aliquots of studied compound stock solutions were added to 5.5 mL of 5×10^{-4} M ct-DNA solution (pH 7, buffer Na cacodylate, $I = 0.05$ M), with ratio $r_{[compound]/[ct\text{-}DNA]} < 0.2$. The flow times were measured at least three times with a deviation of ±0.5 s. The viscosity index α was obtained from the flow times at varying r according to the following equation:[27]

$$L/L_0 = [(t_r - t_0)/(t_{DNA} - t_0)]^{1/3} = 1 + \alpha r$$

t_0, t_{DNA}, and t_r denote the flow times of buffer, free DNA, and DNA complex at ratio $r_{[1]/[ct\text{-}DNA]}$, respectively. L/L_0 is the relative DNA lengthening. The L/L_0 vs r plot (Supporting Information) was fitted to a straight line that gave slope α. The error in α is ±0.1. Under the same conditions, experiments with ethidium bromide (EB) were performed for comparison reasons (Supporting Information).

Antitumor Activity Assays. Antiproliferative Activity. The HeLa (cervical carcinoma), H460 (lung carcinoma), MCF-7 (breast carcinoma), SW620 (colon carcinoma), and MiaPaCa-2 (pancreatic carcinoma) cells (obtained from American Type Culture Collection (ATCC, Rockville, MD) were cultured as monolayers and maintained in Dulbecco's modified Eagle's medium (DMEM) supplemented with 10% fetal bovine serum (FBS), 2 mM L-glutamine, 100 U/mL penicillin, and 100 μg/mL streptomycin in a humidified atmosphere with 5% CO_2 at 37 °C. The growth inhibition activity was assessed as described previously, according to the slightly modified procedure of the National Cancer Institute, Developmental Therapeutics Program.[25−27] Briefly, the cells were cultured as monolayers and maintained in Dulbecco's modified Eagle's medium (DMEM) supplemented with 10% fetal bovine serum (FBS), 2 mM L-glutamine, 100 U mL^{-1} penicillin, and 100 μg mL^{-1} streptomycin in a humidified atmosphere with 5% CO_2 at 37 °C. The cells were inoculated onto a series of standard 96-well microtiter plates on day 0, at 1×10^4 to 3×10^4 cells/mL, depending on the doubling times of the specific cell line. Test agents were then added in five serial 10-fold dilutions (10^{-8}−10^{-4} M) and incubated for a further 72 h. Working dilutions were freshly prepared on the day of testing. The solvent (DMSO) was also tested for eventual inhibitory activity by adjusting its concentration to be the same as in the working concentrations. The cell growth rate was evaluated by performing the MTT assay after 72 h of incubation, which detects mitochondrial dehydrogenase activity in viable cells.

Each test was performed in quadruplicate in three individual experiments. The results are expressed as IC_{50}, which is the concentration necessary for 50% of inhibition. The IC_{50} values for each compound are calculated from concentration−response curves using linear regression analysis by fitting the test concentrations that give PG values above and below the reference value (i.e., 50%). If, however, for a given cell line all of the tested concentrations produce PGs exceeding the respective reference level of effect (e.g., PG value of 50), then the highest tested concentration is assigned as the default measurment value, which is preceded by a ">" sign preceding the number.

Cell Cycle Analysis. Tumor cells (2×10^5) were seeded per well into a six-well plate. After 24 h the tested compounds were added at various concentrations (as shown in the results section). After the desired length of time the attached cells were trypsinized, combined with floating cells, washed with phosphate buffer saline (PBS), fixed with 70% ethanol, and stored at −20 °C. Immediately before the analysis, the cells were washed with

PBS and stained with 50 μg/mL propidium iodide (PI) with the addition of 0.2 μg/μL RNase A. The stained cells were then analyzed with Becton Dickinson FACScalibur (Becton Dickenson) flow cytometer (20 000 counts were measured). The percentage of the cells in each cell cycle phase was determined using the ModFit LT software (Verity Software House) based on the DNA histograms. The tests were performed in duplicate and repeated at least twice.

Topoisomerase I DNA Unwinding/Cleavage Assay. In vitro assay using purified calf thymus topoisomerase I (Invitrogen) was used in order to check selected compounds for their inhibitory effect on topoisomerase I according to Bailly,[34] whereby two possible modes of inhibition can be detected: nonspecific effect, due to DNA intercalation, and specific effects resulting from the poisoning of topoisomerase I. Briefly, the reaction mixture contained 0.8 μg of negatively supercoiled plasmid pCI (Promega, kindly provided by Dr. Andreja Ambriović Ristov, Ruđer Bošković Institute, Zagreb, Croatia) and 6 U of topoisomerase I, with or without tested inhibitors in 40 μL of relaxation buffer (10 mM Tris-HCl, pH 7.5, 175 mM KCl, 5 mM $MgCl_2$, 0.1 mM EDTA, 2.5% glycerol). The mixtures were incubated at 37 °C for 30 min, and the reaction was terminated by the addition of 2.5 μL of 10% SDS, followed by proteinase K (50 μg/ml) digestion at 37 °C for 15 min. After extraction with a mixture of phenol, chloroform, and isoamyl alcohol (25:24:1), aqueous samples were removed and an amount of 2 μL of gel-loading buffer (0.25% bromphenol blue, 0.25% xylene cyanol, 60% glycerol, 150 mM Tris, pH 7.6) was added. The samples were divided in two and loaded onto either 1% agarose gel containing 0.5 μg/mL ethidium bromide or 1% agarose gel without ethidium bromide. Gels were run at 80 V constant voltage in a horizontal electrophoresis system (BIO-RAD). Resulting products were visualized and documented with UV light at 254 nm (Uvitec, Cambridge, U.K.).

Cellular Tubulin Staining. MiaPaCa-2 cells (2×10^5) were grown overnight on 18 mm × 18 mm coverslips and placed in each well of the six-well plate. Our tested compounds, paclitaxel (Sigma) and colchicine (Sigma), were then added at various concentrations as described in the results section and Supporting Information. After 24 h, coverslips were washed with PBS and cells were fixed in 4% formaldehyde in PBS for 10 min, washed twice with PBS, and permeabilized with 0.1% Triton-X 100 in PBS for 10 min. Coverslips were than washed with PBS and blocked with 4% FCS in PBS for 30 min. After that, coverslips were incubated with a mouse monoclonal anti-α-tubulin antibody (100 μg/mL, Calbiochem) diluted $^1/_{200}$ in blocking solution for 2 h, washed five times in PBS, and incubated with FITC-goat antimouse IgG/IgM secondary antibody (0.5 mg/mL, BD Pharmingen) diluted $^1/_{500}$ in blocking solution for 1 h. After being washed with PBS, coverslips were washed with water and placed on microscope slide in 1 drop of fluorescence mounting medium (DAKO). DAPI was added to the mounting medium in a final concentration of 100 ng/mL. Immunofluorescence was analyzed on an Olympus BX51 microscope with an Olympus DP51 camera.

Acknowledgment. Support for this study by the Ministry of Science, Education and Sport of Croatia is gratefully acknowledged (Projects 125-0982464-1356, 098-0982464-2514, 98-0982914-2918, 098-0982464-2393). The authors are grateful to Dr. Mirko Hadžija for his assistance at the fluorescence microscope.

Supporting Information Available: Experimental details, spectroscopic data, and elemental analysis results for compounds **4**−**7**, **10**−**13**, and **14**−**17**; spectroscopy details; results of DNA binding studies; additional photos of tubulin immunofluorescence staining of MiaPaCa-2 cells. This material is available free of charge via the Internet at http://pubs.acs.org.

References

(1) Diana, P.; Martorana, A.; Barraja, P.; Montalbano, A.; Dattolo, G.; Cirrincione, G.; Dall'Acqua, F.; Salvador, A.; Vedaldi, D.; Basso, G.; Viola, G. Isoindolo[2,1-*a*]quinoxaline derivatives, novel potent antitumor agents with dual inhibition of tubulin polymerization and topoisomerase I. *J. Med. Chem.* **2008**, *51*, 2387–2399.

(2) Wilson, L.; Jordan, M. A. Microtubule dynamics: taking aim at a moving target. *Chem. Biol.* **1995**, *2*, 569–573.

(3) Magedov, I. V.; Manpadi, M.; Ogasawara, M. A.; Dhawan, A. S.; Rogelj, S.; Van Slambrouck, S.; Steelant, W. F.; Evdokimov, N. M.; Uglinskii, P. Y.; Elias, E. M.; Knee, E. J.; Tongwa, P.; Antipin, M. Y.; Kornienko, A. Structural simplification of bioactive natural products with multicomponent synthesis. 2. Antiproliferative and antitubulin activities of pyrano[3,2-*c*]pyridones and pyrano[3,2-*c*]quinolones. *J. Med. Chem.* **2008**, *51*, 2561–2570.

(4) Letafat, B.; Emami, S.; Mohammadhosseini, N.; Faramarzi, M. A.; Samadi, N.; Shafiee, A.; Foroumadi, A. Synthesis and antibacterial activity of new *N*-[2-(thiophen-3-yl)ethyl]piperazinyl quinolones. *Chem. Pharm. Bull.* **2007**, *55*, 894–898.

(5) Wang, S. W.; Pan, S. L.; Huang, Y. C.; Guh, J. H.; Chiang, P. C.; Huang, D. Y.; Kuo, S. C.; Lee, K. H.; Teng, C. M. CHM-1, a novel synthetic quinolone with potent and selective antimitotic antitumor activity against human hepatocellular carcinoma in vitro and in vivo. *Mol. Cancer Ther.* **2008**, *7*, 350–360.

(6) Hoang, H.; LaBarbera, D. V.; Mohammed, K. A.; Ireland, C. M.; Skibo, E. B. Synthesis and biological evaluation of imidazoquinoxalinones, imidazole analogues of pyrrolo-iminoquinone marine natural products. *J. Med. Chem.* **2007**, *50*, 4561–4571.

(7) Chen, M. H.; Fitzgerald, P.; Singh, S. B.; O'Neill, E. A.; Schwartz, C. D.; Thompson, C. M.; O'Keefe, S. J.; Zaller, D. M.; Doherty, J. B. Synthesis and biological activity of quinolinone and dihydroquinolinone p38 MAP kinase inhibitors. *Bioorg. Med. Chem. Lett.* **2008**, *18*, 2222–2226.

(8) Srivastava, S. K.; Jha, A.; Agarwal, S. K.; Mukherjee, R.; Burman, A. C. Synthesis and structure−activity relationships of potent antitumor active quinoline and naphthyridine derivatives. *Anti-Cancer Agents Med. Chem.* **2007**, *7*, 685–709.

(9) Deady, L. W.; Rogers, M. L.; Zhuang, L.; Baguley, B. C.; Denny, W. A. Synthesis and cytotoxic activity of carboxamide derivatives of benzo[*b*][1,6]naphthyridin-(5*H*)ones. *Bioorg. Med. Chem.* **2005**, *13*, 1341–1355.

(10) Swaminathan, R.; Natarajan, P. L.; Levorsea, M.; Thompsonb, J. E.; O'Neillb, E. A.; O'Keefeb, S. J.; Vorab, K. A.; Cvetovichc, R.; Chungc, J. Y.; Carballo-Jane, E.; Visco, D. M. P38 MAP kinase inhibitors. Part 5: Discovery of an orally bio-available and highly efficacious compound based on the 7-amino-naphthyridone scaffold. *Bioorg. Med. Chem. Lett.* **2006**, *16*, 5468–5471.

(11) Bilodeau, M. T.; et al. Allosteric inhibitors of Akt1 and Akt2: a naphthyridinone with efficacy in an A2780 tumor xenograft model. *Bioorg. Med. Chem. Lett.* **2008**, *18*, 3178–3182.

(12) Ruchelman, A. L.; Zhu, S.; Zhou, N.; Liu, A.; Liu, L. F.; LaVoie, E. J. Dimethoxybenzo[*i*]phenanthridine-12-carboxylic acid derivatives and 6*H*-dibenzo[*c*,*h*][2,6]naphthyridin-5-ones with potent topoisomerase I-targeting activity and cytotoxicity. *Bioorg. Med. Chem. Lett.* **2004**, *14*, 5585–5589.

(13) Ruchelman, A. L.; Kerrigan, J. E.; Li, T. K.; Zhou, N.; Liu, A.; Liu, L. F.; LaVoie, E. J. Nitro and amino substitution within the A-ring of 5*H*-8,9-dimethoxy-5-(2-*N*,*N*-dimethylaminoethyl) dibenzo[*c*,*h*][1,6]-naphthyridin-6-ones: influence on topoisomerase I-targeting activity and cytotoxicity. *Bioorg. Med. Chem.* **2004**, *13*, 3731–3742.

(14) Kerrigan, J. E.; Pilch, D. S.; Ruchelman, A. L.; Zhou, N.; Liu, A.; Liu, L. F.; LaVoie, E. J. 5*H*-8,9-Dimethoxy-5-(2-*N*,*N*-dimethylaminoethyl)dibenzo[*c*,*h*][1,6]naphthyridin-6-ones and related compounds as TOP1-targeting agents: influence of structure on the ternary cleavable complex formation. *Bioorg. Med. Chem. Lett.* **2003**, *13*, 3395–3399.

(15) Deady, L. W.; Rodemann, T.; Zhuang, L.; Baguley, B. C.; Denny, W. A. Synthesis and cytotoxic activity of carboxamide derivatives of benzo[*b*][1,6]naphthyridines. *J. Med. Chem.* **2003**, *46*, 1049–1054.

(16) Hinman, M. M.; Rosenberg, T. A.; Balli, D.; Black-Schaefer, C.; Chovan, L. E.; Kalvin, D.; Merta, P. J.; Nilius, A. M.; Pratt, S. D.; Soni, N. B.; Wagenaar, F. L.; Weitzberg, M.; Wagner, R.; Beutel, B. A. Novel antibacterial class: a series of tetracyclic derivatives. *J. Med. Chem.* **2006**, *49*, 4842–2856.

(17) Buurman, E. T.; Johnson, K. D.; Kelly, R. K.; MacCormack, K. Different modes of action of naphthyridones in Gram-positive and Gram-negative bacteria. *Antimicrob. Agents Chemother.* **2006**, *50*, 385–387.

(18) Tabart, M.; Picaut, G.; Desconclois, J. F.; Dutka-Malen, S.; Huet, Y.; Berthaud, N. Synthesis and biological evaluation of benzo[*b*]naphthyridones, a series of new topical antibacterial agents. *Bioorg. Med. Chem. Lett.* **2001**, *11*, 919–921.

(19) Dogan Koruznjak, J.; Slade, N.; Zamola, B.; Pavelić, K.; Karminski-Zamola, G. Synthesis, photochemical synthesis and antitumor evaluation of novel derivatives of thieno[3′,2′: 4,5]thieno[2,3-c]quinolones. *Chem. Pharm. Bull.* **2002**, *50*, 656–660.

(20) Dogan Koruznjak, J.; Grdiša, M.; Slade, N.; Zamola, B.; Pavelić, K.; Karminski-Zamola, G. Novel derivatives of benzo[*b*]thieno[2,3-*c*]-quinolones: synthesis, photochemical synthesis and antitumor evaluation. *J. Med. Chem.* **2003**, *45*, 4516–4524.
(21) Jarak, I.; Kralj, M.; Šuman, L.; Pavlović, G.; Dogan, J.; Piantanida, I.; Žinić, M.; Pavelić, K.; Karminski-Zamola, G. Novel cyano- and *N*-isopropylamidino-substituted derivatives of benzo[*b*]thiophene-2-carboxanilides and benzo[*b*]thieno[2,3-*c*]quinolones: synthesis, photochemical synthesis, crystal structure determination and antitumor evaluation. Part 2. *J. Med. Chem.* **2005**, *48*, 2346–2360.
(22) Baraldi, P. G.; Bovero, A.; Fruttarolo, F.; Preti, D.; Tabrizi, M. A.; Pavani, M. G.; Romagnoli, R. DNA minor groove binders as potential antitumor and antimicrobial agents. *Med. Res. Rev.* **2004**, *24*, 475–528.
(23) Štarčević, K.; Karminski-Zamola, G.; Piantanida, I.; Žinić, M.; Šuman, L.; Kralj, M. Photoinduced switch of a DNA/RNA inactive molecule into a classical intercalator. *J. Am. Chem. Soc.* **2005**, *127*, 1074–1075.
(24) Bielawska, A.; Bielawski, K.; Anchim, T. Amidine analogues of melphalan: synthesis, cytotoxic activity, and DNA binding properties. *Arch. Pharm. Chem. Life Sci.* **2007**, *340*, 251–257.
(25) Jarak, I.; Kralj, M.; Piantanida, I.; Šuman, L.; Žinić, M.; Pavelić, K.; Karminski-Zamola, G. Novel cyano- and amidino-substituted derivatives of thieno[2,3-*b*]- and thieno[3,2-*b*]thiophene-2-carboxanilides and thieno[3′,2′:4,5]thieno- and thieno[2′,3′:4,5]thieno[2,3-*c*]quinolones: synthesis, photochemical synthesis, DNA binding and antitumor evaluation. *Bioorg. Med. Chem.* **2006**, *14*, 2859–2868.
(26) Hranjec, M.; Kralj, M.; Piantanida, I.; Sedić, M.; Šuman, L.; Pavelić, K.; Karminski-Zamola, G. Novel cyano- and amidino-substituted derivatives of styryl-2-benzimidazoles and benzimidazo[1,2-*a*]quinolines. Synthesis, photochemical synthesis, DNA binding and antitumor evaluation, Part 3. *J. Med. Chem.* **2007**, *50*, 5696–5711.
(27) Hranjec, M.; Piantanida, I.; Kralj, M.; Šuman, L.; Pavelić, K.; Karminski-Zamola, G. Novel amidino-substituted thienyl- and furylvinyl-benzimidazole derivatives and their photochemical conversion into corresponding diaza-cyclopenta[c]fluorenes. Synthesis, interactions with DNA and RNA and antitumor evaluation. Part 4. *J. Med. Chem.* **2008**, *51*, 4899–4910.
(28) (a) Scatchard, G. *Ann. N.Y. Acad. Sci.* **1949**, *51*, 660. (b) McGhee, J. D.; von Hippel, P. H. *J. Mol. Biol.* **1976**, *103*, 679.
(29) Rodger, A.; Norden, B. In *Circular Dichroism and Linear Dichroism*; Oxford University Press: New York, 1997.
(30) Berova, N.; Nakanishi, K.; Woody, R. W. In *Circular Dichroism Principles and Applications*, 2nd ed.; Wiley-VCH: New York, 2000.
(31) Eriksson, M.; Nordén, B. *Methods Enzymol.* **2001**, *340*, 68.
(32) Kasibhatla, S.; Baichwal, V.; Sui Xiong, C.; Roth, B.; Skvortsova, I.; Skvortsov, S.; Lukas, P.; English, N. M.; Sirisoma, N.; Drewe, J.; Pervin, A.; Tseng, B.; Carlson, R. O.; Pleiman, C. M. MPC-6827: a small-molecule inhibitor of microtubule formation that is not a substrate for multidrug resistance pumps. *Cancer Res.* **2007**, *67*, 5865–5871.
(33) Bhalla, K. N. Microtubule-targeted anticancer agents and apoptosis. *Oncogene* **2003**, *22*, 9075–9086.
(34) Bailly, C. DNA relaxation and cleavage assays to study topoisomerase I inhibitors. *Methods Enzymol.* **2001**, *340*, 610–623.
(35) Sappal, D. S.; McClendon, A. K.; Fleming, J. A.; Thoroddsen, V.; Connolly, K.; Reimer, C.; Blackman, R. K.; Bulawa, C. E.; Osheroff, N.; Charlton, P.; Rudolph-Owen, L. A. Biological characterization of MLN944: a potent DNA binding agent. *Mol. Cancer Ther.* **2004**, *3*, 47–58.
(36) Chen, A. Y.; Yu, C.; Gatto, B.; Liu, L. F. DNA minor groove-binding ligands: a different class of mammalian DNA topoisomerase I inhibitors. *Proc. Natl. Acad. Sci. U.S.A.* **1993**, *90*, 8131–8135.
(37) McKnight, R. E.; Onogul, B.; Polasani, S. R.; Gannon, M. K.; Detty, M. R. Substituent control of DNA binding modes in a series of chalcogenoxanthylium photosensitizers as determined by isothermal titration calorimetry and topoisomerase I DNA unwinding assay. *Bioorg. Med. Chem.* **2008**, *16*, 10221–10227.
(38) Hsiao, C. J.; Ho, Y. F.; Hsu, J. T.; Chang, W. L.; Chen, Y. C.; Shen, Y. C.; Lyu, P. C.; Guh, J. H. Mana-Hox displays anticancer activity against prostate cancer cells through tubulin depolymerization and DNA damage stress. *Naunyn Schmiedeberg's Arch. Pharmacol.* **2008**, *378*, 599–608.
(39) Roninson, I. B.; Broude, E. V.; Chang, B. D. If not apoptosis, then what? Treatment-induced senescence and mitotic catastrophe in tumor cells. *Drug Resist. Updates* **2001**, *4*, 303–313.
(40) (a) Chaires, J. B.; Dattagupta, N.; Crothers, D. M. Studies on interaction of anthracycline antibiotics and deoxyribonucleic acid: equilibrium binding studies on the interaction of daunomycin with deoxyribonucleic acid. *Biochemistry* **1982**, *21*, 3933–3940. (b) Palm, B. S.; Piantanida, I.; Žinić, M.; Schneider, H. J. The interaction of new 4,9-diazapyrenium compounds with double stranded nucleic acids. *J. Chem. Soc., Perkin Trans. 2* **2000**, 385–392.

JM801573V